# Role of Self-Assembly Conditions and Amphiphilic Balance on Nanoparticle Formation of PEG-PDLLA Copolymers in Aqueous Environments

**Hien Phan,[1,2] Robert I. Minut,[2,3] Phoebe McCrorie,[2] Catherine Vasey,[2] Ryan R. Larder,[4] Eduards Krumins,[4] Maria Marlow,[3] Ruman Rahman,[5] Cameron Alexander,[2] Vincenzo Taresco,[2,4] Amanda K. Pearce[2,6]**

[1]Faculty of Pharmacy, University of Angers, 49035 Angers, France
[2]School of Pharmacy, University of Nottingham, Nottingham NG7 2RD, United Kingdom
[3]Department of Pharmacy, D'Annunzio University of Chieti–Pescara, 66100 Chieti, Italy
[4]School of Chemistry, University of Nottingham, Nottingham NG7 2RD, United Kingdom
[5]Faculty of Medicine & Health Sciences, University of Nottingham, Nottingham NG7 2RD, United Kingdom
[6]School of Chemistry, University of Birmingham, Birmingham B15 2TT, United Kingdom
Correspondence to: V. Taresco (E-mail: vincenzo.taresco@nottingham.ac.uk) or A. K. Pearce (E-mail: a.k.pearce@bham.ac.uk)

Received 2 July 2019; Revised 18 July 2019; accepted 19 July 2019
**DOI: 10.1002/pola.29451**

**ABSTRACT**: The production of well-defined and reproducible polymeric nanoparticles (NPs), in terms of size and stability in biological environments, is undoubtedly a fundamental challenge in the formulation of novel and more effective nanomedicines. The adoption of PEGylated lactide (LA) block copolymers as biodegradable and biocompatible nanocarriers at different clinical stages has rendered these materials an attractive polymeric platform to be exploited and their formulation is further understood. In the present work, we synthesized a library of linear polyethylene glycol-poly(D,L-lactide) block copolymers with different lengths of LA (15, 25, 50, and 100 LA units) via simple and metal-free ring-opening polymerization, in order to alter the amphiphilic balance of the different macromolecules. The produced polymers were formulated into NPs while varying a series of key parameters in the solvent displacement process, including solvent:nonsolvent ratios and the nature of the two media, and the effect on size and stability was assessed. In addition, stability to protein–NPs interaction and aggregation was studied, highlighting the different NP final properties according to the nature of the amphiphilic balance and nanoformulation conditions. Therefore, we have illustrated a systematic and methodological process to optimize a series of NPs parameters balancing particle size, size distribution, surface charge, and stability to guide future works in the nanoformulation field. © 2019 The Authors. *Journal of Polymer Science Part A: Polymer Chemistry* published by Wiley Periodicals, Inc. J. Polym. Sci., Part A: Polym. Chem. **2019**

**KEYWORDS**: block copolymers; nanoformulation; NP size; NP stability; PEG-PDLLA

**INTRODUCTION** The use of nanoparticles (NPs) for drug delivery is a rapidly growing field, with nanomedicines showing great promise to improve the clinical outcomes for a range of diseases.[1] Encapsulation or tethering of small molecule therapeutics within NPs can result in improved solubility, stability, and blood circulation times, and ultimately enhance bioavailability.[2] Polymeric NPs are of particular interest as their physicochemical properties can be readily tuned, allowing the polymer structure and chemistry, as well as ultimate NP size and stability, to be modified on demand to precisely meet the requirements of each application.[3] In this regard, tailoring the size of NPs is a crucial design strategy, as physical size can dictate the *in vivo* fate of NPs following administration. For systemic administration, controlling the NP size to within circa 5–200 nm minimizes the premature clearance of particles through renal filtration (<5 nm) or by excessive liver and spleen accumulation (>200 nm).[4,5] In addition, studies have shown that controlling particle size to less than 100 nm can aid prevention of serum protein attachment, thus enhancing NP stability and prolonging blood half-lives.[6] In cancer drug delivery, the long circulation times of large-sized NPs further improve preferential accumulation within tumor sites as a result of enhanced permeation through leaky blood vessels, typical for rapidly growing solid tumors.[7] On the other hand, smaller sized NPs (<50 nm) show

Additional supporting information may be found in the online version of this article.

enhanced extravasation, tissue penetration across multiple cell layers, and cellular uptake, particularly in the cases of slow-growing or heterogeneous tumors that do not present with significant vascular fenestrations.[8–10] Finally, size requirements for NPs to cross biological barriers such as the blood–brain barrier, or for targeting toward specific organs, are also factors to be accounted for in NP design.[11,12] Therefore, it is imperative to be able to precisely tune the physical characteristics of the nanomedicine carrier for each specific drug delivery scenario.

Critically, in the interests of ultimate translation of nanomedicines into the clinic, one of the main challenges to be overcome is the ability to achieve these tailored aspects of polymeric NPs, while at the same time facilitating scalability and cost-effectiveness for the pharmaceutical industry. It is of crucial importance to reduce synthetic complexity, tedious purification steps, the number of different components, and addition of toxic surfactants in order to maintain batch-to-batch consistency, clinical relevance, and patient safety. One widely used approach in this regard is to employ amphiphilic block copolymers as the carrier materials, as they can inherently self-assemble into NPs in an aqueous environment without the use of additional stabilizers. Specifically, incorporating hydrophilic segments such as polyethylene glycol (PEG) provides a hydrophilic corona that can impart the final formulation with stability in biological environments, and biodegradable hydrophobic segments, such as D,L-lactide (LA) and D,L-LA-co-glycolide, provide a hydrophobic core region that can facilitate encapsulation and release of active agents. This strategy is well exemplified by several clinically relevant nanomedicines based on poly(D,L-lactide) (PDLLA), including the FDA-approved Genexol-PM for delivery of paclitaxel, and the BIND-014 and Accurins technologies currently in Phase I and II clinical trials.[6,13,14]

PDLLA and its copolymers are routinely synthesized through ring-opening polymerization (ROP); a powerful, simple, and versatile technique. However, a major drawback with LA-based polymers and copolymers is the toxic catalyst and stringent reaction conditions typically utilized in their production.[15–17] Recently, we demonstrated a more friendly catalytic approach for ROP of LA in ambient conditions and at room temperature,[18–20] using mild organocatalysts such as 1,8-diazabicyclo[5.4.0]undec-5-ene (DBU).[21–24] This synthetic approach negates the need for toxic catalysts, high temperature reactions (over 120°C), and more extensive purifications, thereby facilitating further access to these materials across nonspecialist chemical laboratories.

Employing PEG as the ROP initiator results in the production of amphiphilic materials in a single step, where the ratio of the hydrophilic and hydrophobic components can be readily tuned. Due to their intrinsic amphiphilic balance, PEGylated block copolymers are perfect candidates to be formulated into NPs via simple nanoprecipitation techniques. In this regard, previous studies have demonstrated that the amphiphilic balance of the copolymers can impact the size, stability, surface charge, and protein corona formation on the final NPs.[25] However, there are a series of physicochemical parameters that drive the nucleation, growth, and aggregation of the polymers into NPs during the nanoprecipitation process that have not yet been fully understood.[26] Comprehension of the relationship between these parameters and their quantitative effects on NP formation via nanoprecipitation could be an invaluable tool in the translation of this methodology on a larger scale.

Based on this, in the present work, we aimed to systematically study the factors that influence the nanoformulation process of PEG-PDLLA copolymers. The ability to modulate, on demand, the final NP size and stability simply through tuning the formulation parameters is a potential strategy to achieve optimum physical characteristics without requiring the synthesis of new polymers each time. While investigations into the self-assembly behavior of PLGA and PCL polymers have been analyzed and reported in detail in previous literature,[26–29] as well as one example of a PEGylated block copolymer (poly(ethylene glycol)-*b*-poly(*N*-2-benzoyloxypropyl methacrylamide) (mPEG-*b*-p(HPMA-Bz)), to our knowledge, this process has not been explored in detail for PEG-PDLLA polymers.[30] Therefore, to provide important insights into the tunable parameters that influence self-assembly of these clinically relevant materials, this work presents a complete study of NP formation and assessment of stability. We screened the self-assembly, NP size, and stability of a library of PEG-PDLLA copolymers with varied lengths of the hydrophilic and hydrophobic blocks, evaluating the magnitude of impact of changing the amphiphilic balance of the polymer and the precipitation solvent, nonsolvent, and their respective ratios. In addition, with the intention to expand the screening procedure toward prebiological *in vitro* evaluation, we developed a DLS-based assay to assess the stability of the resultant NPs against protein-induced aggregation using bovine serum albumin (BSA) as a model serum protein.[31] Therefore, this work provides vital and concise strategies for modulating NPs formation from a highly exploited polymeric material such as PEG-PDLLA, for a variety of self-assembly and pharmaceutical applications.

## EXPERIMENTAL

### Materials

Poly(ethylene glycol) methyl ether ($M_n$ = 5000 or 2000 Da) and DBU (98%) were purchased from Sigma-Aldrich, UK. Dichloromethane (DCM, 99.8%, extra dry over molecular sieve, stabilized, Acroseal) was purchased from AcrosOrganics, UK. DL-LA (99%), acetone, acetonitrile (ACN), and THF were purchased from Fisher Scientific, UK. All chemicals were used as obtained without additional purification unless otherwise stated.

### PEG-Initiated Ring-Opening Polymerization of Lactide Block Copolymer

A representative synthesis of $mPEG_{5000}$-$LA_{15}$ was as follows. A predetermined amount of PEGylated chain initiator and DL-LA were directly weighed out (1.00 g of LA and 2.31 g of $mPEG_{5000}$) in a glass vial (dried in an oven at 100°C overnight) and capped. Dry DCM (5 mL) was added and the mixture was allowed to dissolve at room temperature. DBU (3% w/w with respect to the amount of LA) was directly added to the reaction mixture to catalyze the ROP. After 15 min, the

polymerization was quenched by adding the solution dropwise into cold hexane (30 mL) and the polymer was purified via multiple precipitation steps in hexane and diethyl ether. Finally, the polymer was dried under vacuum (conversion of monomer into polymer ~75–80% w/w). A final NMR spectrum was recorded of the products postpurification. The library of copolymers were achieved by adjusting the initial [M]/[I] ratio in order to target the desired length of LA. $^1$H NMR (400 MHz, $CDCl_3$, ppm): $\delta$ 5.19 (broad m, xH), 3.67 (broad s, 356H), 3.3 (x) 1.65–1.47 (2 asymmetric broad s, 53 + 78H).

### Nanoparticle Preparation

A nanoprecipitation, or solvent displacement, method was used to form NPs. In particular, polymer (10 mg) was dissolved in either acetone, THF, or ACN (volume adjusted according to the organic solvent/aqueous medium ratio). The polymeric solution was added either by hand or by an automatic pump to deionized water (10 mL, within 30 s), under constant stirring at 550 rpm. The polymers rapidly formed NP suspensions through solvent exchange between the aqueous medium and the organic solvents. The final suspension was then left stirring for 24 h at room temperature in order to reach complete organic solvent removal via evaporation.

### Protein Binding Assay

To determine protein corona association to the NPs, binding studies were undertaken using BSA as the model protein. Each NP (1 mg/mL in PBS) and BSA alone (2 mg/mL in PBS) was sized by DLS at a fixed attenuation. BSA was added (150 μL) to NPs (150 μL) (final conc. NPs:500 μg/mL, BSA: 0.2 wt % [equivalent to culture media+10% FBS]). The samples were incubated at 37°C and size measurements of the samples were taken by DLS on a Zetasizer after 1, 24, and 48 h. BSA was prepared as a stock solution in PBS at 4 mg/mL.

### General Methods and Instrumentation

*NMR*: Bruker AV400 and AV3400 NMR spectrometers operating at 400 MHz ($^1$H) and 101 MHz ($^{13}$C) at ambient temperature were used to perform NMR analysis in deuterated solvents. Chemical shifts were assigned in parts per million (ppm). $^1$H NMR chemical shifts ($\delta_H$) are reported with the shift of C*H*$Cl_3$ ($\delta$ = 7.26 ppm) as the internal standard when $CDCl_3$ was used. $^{13}$C Chemical shifts ($\delta_C$) are reported using the central line of *C*H$Cl_3$ ($\delta$ = 77.0 ppm) as the internal standard. All spectra were obtained at ambient temperature (22°C ± 1°C). MestReNova 6.0.2 copyright 2009 (Mestrelab Research S. L.) was used for analyzing the spectra.

*FTIR*: FTIR spectroscopy was performed in the range of 4000–650 cm$^{-1}$. This was carried out using a Bruker Tensor 27 FTIR spectrophotometer using an ATR attachment. Spectra were analyzed using the MicroLab software.

*GPC*: GPC was used for determination of number average molecular weight ($M_n$), weight average molecular weight ($M_w$), peak molecular weight ($M_p$), and molecular weight distribution (dispersity, Đ, $M_w/M_n$). The analysis was performed using an Agilent 1260 Infinity Series HPLC (Agilent Technologies) fitted with two Agilent PL-gel Mixed-C columns in series at a flow rate of 1 mL min$^{-1}$ using THF (HPLC grade, Fisher Scientific) as eluent at room temperature and a differential refractive index detector. Poly(methyl methacrylate) standards ($M_n$ range: 1,800,000–505 g mol$^{-1}$) and polycaprolactone standards were used for calibration.

*DSC*: Thermal properties of the materials were studied by DSC (Q2000, TA Instruments, Leatherhead, UK) at a heating rate of 10°C/min.

*DLS*: The particle size and zeta-potential were analyzed by DLS using a Zetasizer Nano ZS (Malvern Instruments Ltd). Measurements were taken in triplicate of NPs suspensions at 1 mg/mL in milliQ water and used to calculate average intensity particle size distributions.

*TEM*: TEM samples were prepared as follows; the sample in aqueous suspension (13 μL) was added to a copper grid (Formvar/carbon film 200 mesh copper [100]). The sample was left on the grid for 10 min and then the excess was removed using filter paper. The grid was allowed to dry under a fume hood for a minimum of 30 min prior to use. TEM images were captured using the FEI Biotwin-12 TEM equipped with a digital camera at the Nanoscale and Microscale Research Centre of the University of Nottingham.

## RESULTS AND DISCUSSION

### Polymer Synthesis and Characterization

A metal-free ROP synthetic strategy catalyzed by DBU in ambient conditions was employed for the synthesis of PEGylated block copolymers, in order to generate amphiphilic copolymers in a single, fast, reaction step with minimal purification requirements (Fig. 1A). Two different mPEG chains, $mPEG_{2000}$ and $mPEG_{5000}$, were used as macroinitiators to produce a library of mPEG-PDLLA block copolymers, varying the initiator to monomer ratios to generate different LA chain lengths, namely 15, 25, 50, and 100 LA units. Monomers reached quantitative conversion into polymers (>98% mol/mol) within 15 mins, independently of the length of the initiator and the monomer/initiator ratio. The resultant polymers were fully characterized, with $^1$H NMR of the purified copolymers showing the characteristic peaks of the polymerized LA in agreement with the monomer and initiator feed ratios as reported in Table 1 and Supporting Information Figure S1. Figure 1C depicts a representative series of stacked $^1$H NMR spectra to exemplify the nature of the typical peaks. In addition, the ATR-IR spectra show all the characteristic transitions of alkyl, ester, and ether moieties, further confirming the successful copolymerization (Fig. 1B). Control of the polymerization in terms of final molecular weight (in close agreement with the number of units observed in the $^1$H NMR spectra) and dispersity (all the values <1.2) was confirmed by GPC analysis, as reported in Table 1 and Supporting Information Figure S2. Thermal analysis of the block copolymers was performed using DSC with one single heating ramp and was carried out from −20 to 120°, and for all the block copolymers, a single endothermal peak was

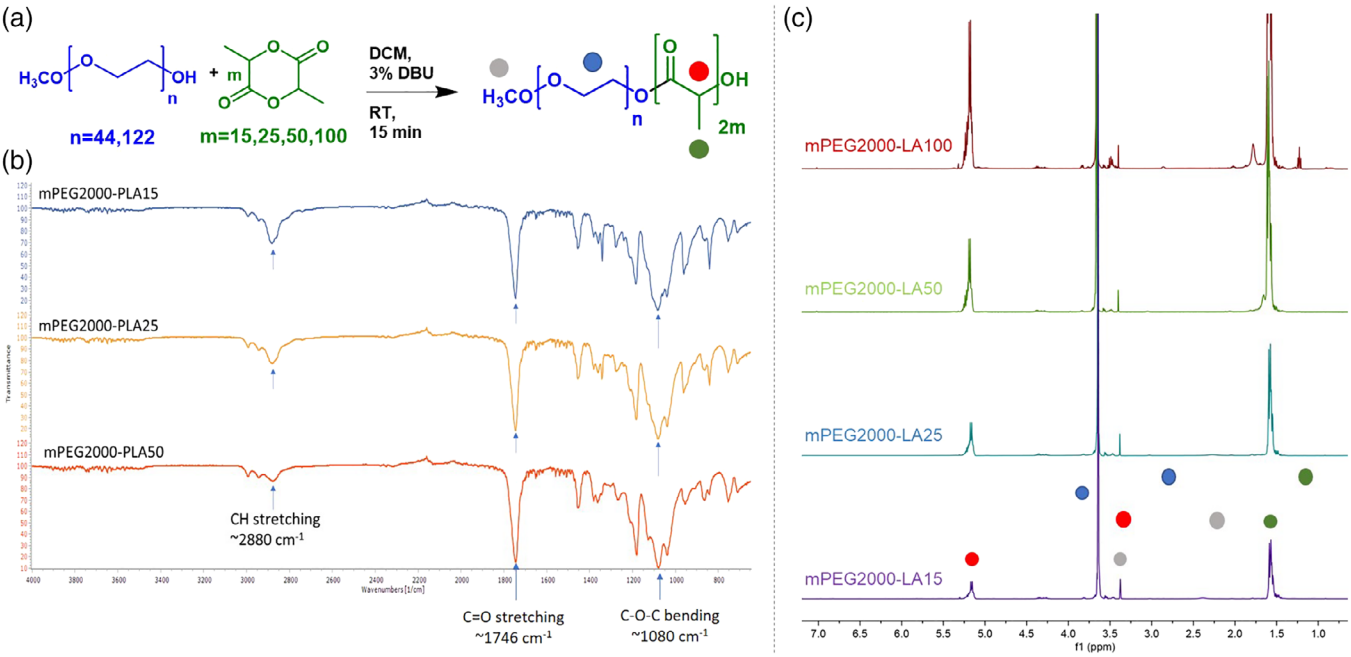


**FIGURE 1** (A) Reaction scheme for DBU-catalyzed mPEG-OH-initiated LA polymerization. (B) ATR-IR stacked spectra of three PEGylated copolymers as examples of the library of materials; main characteristic vibrations are underlined. (C) $^{1}$HNMR stacked spectra of the entire $mPEG_{2000}$ subset of purified block copolymers; main characteristic peaks are highlighted. [Color figure can be viewed at wileyonlinelibrary.com]

observed (Supporting Information Fig. S3). The $T_m$ values calculated from the DSC thermographs are presented in Table 1, where the polymers were observed to have melting points due to the crystalline nature of the PEG initiators (Supporting Information Fig. S3). The melting temperatures gradually decreased on trend with increasing LA chain length, which was attributed to the amorphous and hydrophobic PDLLA chains hindering the chain-packing nucleation step during the cooling cycle. No clear glass transitions could be observed, likely due to the sharp and intense melting transition obscuring the $T_g$ step.

### Evaluation of Varying Formulation Approach and Concentration on Nanoparticles Size

With the view to simplify and validate the formulation strategy in this work, an experiment was performed to compare the formation and final size of the nanoaggregates as a result of nanoprecipitation by syringe pump versus by hand-held pipetting (Fig. 2A). The block copolymers $mPEG_{2000}$-$LA_{100}$ and $mPEG_{5000}$-$LA_{100}$ were used as the representative polymers for this experiment, with nanoprecipitation from acetone into $H_2O$ (final concentration of 1.

mg/mL). Figure 2A depicts the NPs size from both processes as measured by DLS, confirming that the particles produced had no statistical difference in final size within the same subset. The absence of any variations in the average size aligns with previously reported observations[32] when the traditional hand-held process was compared with a fully miniaturized printing approach. This observation may be attributed to the small volume of organic solvent adopted (1–2 mL) per formulation, as well as the high rate of addition to the aqueous

**TABLE 1** Chemical Characterization of the PEGylated Copolymers

| Copolymer | Feed Ratio (PEG:LA) mol % | Composition ($^{1}$H NMR) (PEG:LA) mol % | $M_n$ ($^{1}$H NMR) (Da) | $M_n$ (GPC) (Da)[a] | Đ (SEC) | %PEG/PLA (hydrophilic wt%) | $T_m$ (°C) |
|---|---|---|---|---|---|---|---|
| $mPEG_{2000}$-$LA_{15}$ | 1:15 | 1:16 | 4300 | 7300 | 1.2 | 48 | 47.0 |
| $mPEG_{2000}$-$LA_{25}$ | 1:25 | 1:26 | 5700 | 13,500 | 1.2 | 36 | 45.9 |
| $mPEG_{2000}$-$LA_{50}$ | 1:50 | 1:51 | 9300 | 14,700 | 1.1 | 22 | 43.7 |
| $mPEG_{2000}$-$LA_{100}$ | 1:100 | 1:102 | 17,000 | 20,000 | 1.2 | 12 | 41.6 |
| $mPEG_{5000}$-$LA_{15}$ | 1:15 | 1:15 | 8300 | 8300 | 1.2 | 70 | 58.4 |
| $mPEG_{5000}$-$LA_{25}$ | 1:25 | 1:26 | 9000 | 16,000 | 1.1 | 58 | 55.4 |
| $mPEG_{5000}$-$LA_{50}$ | 1:50 | 1:52 | 13,000 | 19,000 | 1.1 | 41 | 54.1 |
| $mPEG_{5000}$-$LA_{100}$ | 1:100 | 1:104 | 20,000 | 24,000 | 1.2 | 26 | 48.4 |

[a] GPC values compared to PMMA standards.

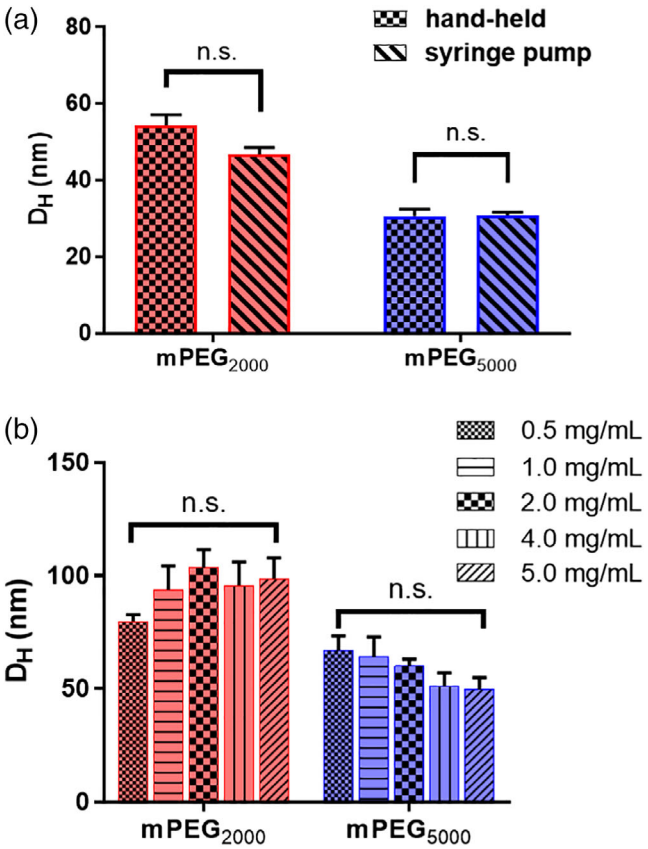


**FIGURE 2** (A) NPs size (nm) of NPs prepared by hand versus by syringe pump; no statistical differences were observed (mean ± SD, error bars represent SD from three different replicate batches). (B) Trend in NPs sizes at different concentrations (from 0.5 to 5 mg/mL) (mean ± SD, error bars represent SD from three different replicate batches). No statistical differences within the $mPEG_{2000}$-$LA_{100}$ and $mPEG_{5000}$-$LA_{100}$ subsets were observed when using a one-way ANOVA with Dunnett's post hoc test ($P < 0.05$). [Color figure can be viewed at wileyonlinelibrary.com]

phase (entire addition process within 30 s). NP sizes were also confirmed to remain unchanged when the final concentration in the aqueous environment was adjusted within an order of magnitude (0.5–5 mg/mL) (Fig. 2B). This behavior was also in agreement with previous work,[32] concerning a series of random and block copolymers nanoformulated within a similar concentration range as explored here. Due to the absence of any concentration effects, a final NP concentration of 1 mg/mL was selected for all future experiments for simplicity. During the NP formation screening process, only formulations that resulted in monomodal samples as measured by DLS were considered to be successful, and therefore reported. Supporting Information Figure S4 demonstrates the typical classification of good (accepted) and poor (rejected) samples to exemplify our applied threshold, and Supporting Information Figure S5 summarizes all of the self-assembly experiments and our applied selection criteria. In this way, any missing values throughout the manuscript represent either a lack of self-assembling or the presence of multiple peaks, unless stated differently.

### Nanoprecipitation from Acetone, THF, and ACN into $H_2O$: Effect of Hydrophobic Block Length and Organic Solvent

The first screening process aimed to identify the relationship between NP sizes when the length of the hydrophobic block was varied from 15 units to 100 units of LA. Additionally, the nanoprecipitation process was performed exploring three different organic solvents (acetone, THF, and ACN) at the same ratio of solvent:nonsolvent (1:5), in order to elucidate any additional solvent effects on the final size and PDI of the NPs. NP measurements were performed a minimum of 24 h after the nanoformulation process in order to ensure full removal of the organic solvent from the final samples. Initially, a series of formulations were prepared and periodically analyzed by DLS over a 72-h period. No change in the NP size or evidence of solvent-induced aggregation was observed during this experiment, thus confirming that all the subsequent analysis was in a pure aqueous environment.

It can be seen in Figure 3 that the LA chain length had a marked effect on the NP size when the PEG length remained unchanged, particularly for the $mPEG_{2000}$ polymer series. NPs assembled from the $mPEG_{2000}$-$LA_{15}$ polymer resulted in NPs of circa 100 nm with a PDI of around 0.2, with small variations in size as the organic solvent was changed (acetone: 88 nm; THF: 101 nm; ACN: 113 nm). However, increasing the size of the LA block to 50 units caused a substantial decrease in NP size to circa 30 nm, while the PDI remained at 0.2. Increasing the length of the hydrophobic block further to 100 units of LA resulted in NPs of a comparable size to the 15 units, but with a decrease in the PDI of the particles down to 0.1, indicating that the longer hydrophobic block may contribute to both the improvement of particle size due to steric effects as well as enhanced LA packing within the NPs core. The $mPEG_{5000}$ series had a similar trend, with the 50 units of LA consistently producing the smallest particle size (circa 30 nm) from all solvents.

However, in this case, the choice of organic solvent had a more tangible effect on the resultant size for the other LA lengths; $mPEG_{5000}$-$LA_{15}$ varied from 35 nm (THF) to 82 nm (ACN), and $mPEG_{5000}$-$LA_{100}$ varied from 35 nm (ACN) to 80 nm (THF). In general, the final PDI values for the $mPEG_{5000}$ series were larger than $mPEG_{2000}$; however, it could still be observed that the 100 units of LA consistently had the smallest PDI. To further explore the solvent effects, the experiments were repeated varying the solvent:nonsolvent ratio to 1:2.5 and 1:1 (Supporting Information Fig. S6). Increasing the amount of organic solvent within the nanoformulation process to 1:1 only produced suitable NPs in certain cases: no stable NPs could be produced from $mPEG_{2000}$-$LA_{50}$ or from ACN in general at this ratio, and THF was successful only for the $mPEG_{5000}$ series. However, the resultant particles were large (>200 nm), although the PDI was narrow (0.04–0.15). Nanoprecipitation from acetone resulted in large particles with a narrow PDI for the $mPEG_{2000}$ polymers (>200 nm, PDI

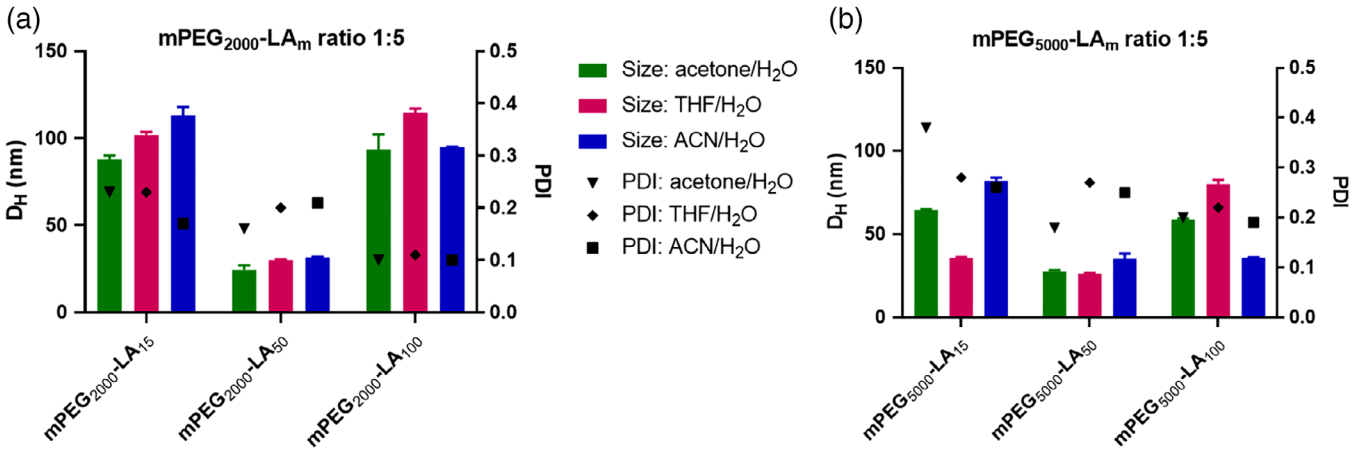


**FIGURE 3** NP size and PDI as an effect of hydrophilic:hydrophobic balance (length of mPEG initiator and units of LA) when nanoformulated in three different solvents at the same solvent:nonsolvent volume ratio (1:5) (mean ± SD, error bars represent SD from three different measurements). Measurements were performed in pure water after full removal of the organic solvent. [Color figure can be viewed at wileyonlinelibrary.com]

<0.12) and large particles with a broad distribution for the $mPEG_{5000}$-$LA_{15}$ (170 nm, PDI 0.4). Small NPs with a broad distribution were produced from the $mPEG_{5000}$ with 25 and 50 units of LA (32 nm, PDI 0.34). The intermediate solvent ratio of 1:2.5 had a less pronounced effect, and particles were produced from all conditions (except for $mPEG_{2000}$-$LA_{50}$ and $mPEG_{5000}$-$LA_{15}$ with ACN). On average, the $mPEG_{2000}$ series had a particle size of >100 nm and a narrow PDI, with the exception of $LA_{50}$, which reduced to around 40 nm. The $mPEG_{5000}$ series had an overall trend of small particle size (25–50 nm) with the exception of $LA_{15}$ at 150 nm from THF, with PDI values varying from 0.08 up to 0.4. From these results, it could be concluded that acetone was the best solvent choice for PEG-LA block copolymers in terms of sizes below 100 nm and PDI below 0.2 for most cases, and that nanoprecipitations performed from a fast addition process resulted in ideal NPs when employing a solvent:nonsolvent ratio of 1:5. However, it was demonstrated that variations in particle size could successfully be obtained from the same polymer simply as a consequence of changing the parameters of nature of organic solvent and solvent:nonsolvent ratio, giving an indication of NP tunability.

### Nanoprecipitation from Acetone, THF, and ACN into PBS: Effect of Presence of Salts

The experimental series from above was next repeated using PBS as the nonsolvent in place of $H_2O$, in order to examine the effect of salt presence on the NP size, as it is known that screening of any surface charges by salts can influence NP size and stability. Figure 4 demonstrates that the overall trend for the $mPEG_{2000}$ series was the production of NPs of approximately 100–150 nm in size, with no significant variations compared with the data from $H_2O$. The solvent ratio of 1:1 (from acetone) increased the NP size to >200 nm, and THF could reduce the NP size to around 40 nm for $LA_{50}$ at the 1:5 and 1:25 ratio. PDI values also showed a similar trend, remaining approximately 0.2–0.3 for most samples. As above, the $mPEG_{5000}$ series produced NPs that were generally smaller than the $mPEG_{2000}$, with most conditions producing particles <80 nm. However, there was also an overall trend of larger particles as a result of nanoprecipitation into PBS compared with $H_2O$. For the $mPEG_{5000}$-$LA_{15}$, the presence of salts within the nonsolvent caused an increase in overall particle size at the 1:5 ratio (acetone: 100 nm, THF: 85 nm, ACN: 150 nm) with the same size trend as in $H_2O$ (acetone: 64 nm, THF: 36 nm, ACN: 82 nm). This was also observed for the $LA_{25}$ at the 1:5 and 1:2.5 ratios, with an increase in the NP size by around 20–50 nm in all conditions.

### Variation in Nanoparticle Zeta Potentials as an Effect of Formulation Conditions

Based on the observations that modifying the organic solvent and solvent:nonsolvent ratios affected the particle size and size distribution, we next investigated how these parameters could also affect surface charge, or zeta potential, of the NPs. The zeta potential is known to influence NP behavior in biological environments, both in terms of stability of the polymer suspension as well as interactions with proteins in the body.[33,34] A slightly negative zeta potential (from neutral to −30 mV) should confer polymeric NPs with resistance to aggregation and reduced interactions with proteins. Zeta potential measurements were performed after nanoprecipitation into milliQ $H_2O$ from acetone, THF, and ACN at the 1:5 and 1:2.5 ratios (Fig. 5). In all the cases, the zeta potential was negative, as expected for PEGylated copolymers; however, the nanoprecipitation conditions could modulate this value from −12 mV down to −33 mV, depending on the polymer. For the $PEG_{2000}$-$LA_{15}$, NPs formed at the 1:5 versus 1:2.5 ratio resulted in the size increasing by up to 50 nm depending on the organic solvent, and this was reflected in a change in zeta potential trending toward neutral (acetone: −22 mV to −12 mV; THF: −19 mV to −16 mV; ACN: −25 mV to −17 mV). In general, nanoprecipitation conditions that produced small particles (less than 50 nm) had the more negative zeta potential. This was observed for the $mPEG_{2000}$-$LA_{50}$, at both 1:5 and1:2.5 ratios,

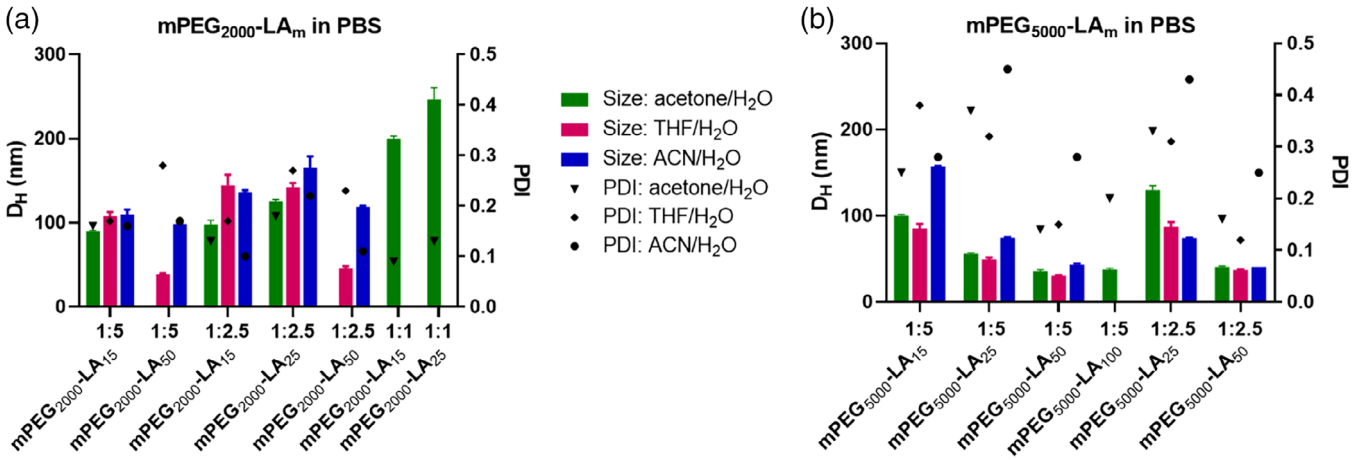


**FIGURE 4** NPs size and PDI as an effect of hydrophilic:hydrophobic balance (length of mPEG initiator and units of LA) when nanoformulated in three different solvents at different solvent:nonsolvent ratios into PBS (mean ± SD, error bars represent SD from three different measurements). Measurements were performed in PBS after full removal of the organic solvent. [Color figure can be viewed at wileyonlinelibrary.com]

where the particle sizes of circa 30 nm had zeta potential values of circa −30 mV.

In contrast, the $mPEG_{2000}$-$LA_{15}$ (hydrophilic 48%) with particle sizes of >100 nm at the 1:2.5 solvent:nonsolvent ratio had a zeta potential of circa −12 mV. There was also a clear correlation between the amphiphilic balance of the block copolymers and the zeta potential, where the block copolymers with a lower hydrophilic block% had more negative surface potentials. This was exemplified for the $mPEG_{2000}$-$LA_{100}$, which had the lowest percentage of PEG (12%) and the lowest zeta potential at circa −33 mV. We speculate that this is a result of the shorter PEG lengths providing a more extended brush conformation on the NP surface, and thus enhanced charge/surface area properties.

### Stability of Nanoparticles in Presence of BSA

Finally, to further evaluate the stability of the produced NPs as an effect of size and surface charge in biologically relevant conditions, a screening assay was developed using DLS with BSA as the model protein to assess protein-induced aggregation.[31] A DLS-based assay was chosen as the preliminary screening technique due to the fast response time and ease of detection of aggregation within each sample. The $mPEG_{2000}$ library (nanoprecipitated from acetone into $H_2O$ ratio 1:5) was selected as representative polymers, to evaluate in comparison with the zeta potential analysis from above.

NPs were incubated with 0.2 wt % of BSA at 37°C to represent protein concentrations within *in vitro* conditions.[35] It could be seen from the DLS traces that all NPs in this experiment initially had monomodal size distributions in accordance with the screening described above. Importantly, the NPs also remained stable over time in the presence of BSA with a little or no observed particle aggregation (Fig. 6). Taking into account the results of surface charge from Figure 5, a correlation between zeta potential and the stability of the particles over time in presence of albumin can be proposed. The $mPEG_{2000}$-$LA_{15}$ had a zeta potential of circa −20 mV, and was observed to be moderately stable from this experiment, with some broadening in the peak after 48 h. However, the 50 and 100 units of LA, with zeta potentials of circa −30 mV, demonstrated improved stability, with virtually unchanged DLS traces over the course of the experiment. As a comparison, we also analyzed the stability of a large particle with broad PDI value, $mPEG_{5000}$-$LA_{15}$ (hydrophilic ratio 70%), to ascertain the impact of a more neutral zeta potential in these conditions (−5.8 mV, data not shown). It can be seen in Supporting Information Figure S7 that this formulation initially had a bimodal size distribution in accordance with the screening experiments above, which likely contributed to the observed instability of the particle in the presence of the BSA during observation. The DLS traces depict evidence of aggregation by 24 h, and increasing by 48 h, potentially as a result of the relatively short core-forming hydrophobic block and reduced charge density as confirmed by the zeta potential close to neutral.

To corroborate this speculation of the link between size, charge density, and narrow PDI on particle stability in the presence of BSA, we finally analyzed the change in zeta potential of the four NPs when exposed to increasing salt conditions (25, 150, and 250 μg/mL NaCl). PEGylated polymers typically demonstrate a negative zeta potential arising from cations associating with the oxygen lone pairs on the PEG chain causing a loose surface shell of counter anions when in solution. Addition of NaCl screens these surface charges, causing the zeta potential to neutralize.[36] A trend between the zeta potential in pure water and rate and extent at which the surface charge neutralized could be observed between the four NPs. It was observed that the $mPEG_{5000}$-$LA_{15}$ that was not stable to BSA had a rapid change with increasing concentration of NaCl and reached 97% of neutralization. Importantly, the $mPEG_{2000}$ with 50 and 100 units of LA, with starting zeta potentials of circa −30 mV, showed the slowest change over NaCl concentration, reaching a final neutralization of 87% (Supporting Information Fig. S8). The $mPEG_{2000}$-$LA_{15}$, starting from −22 mV, showed a slightly more rapid neutralization; however, it

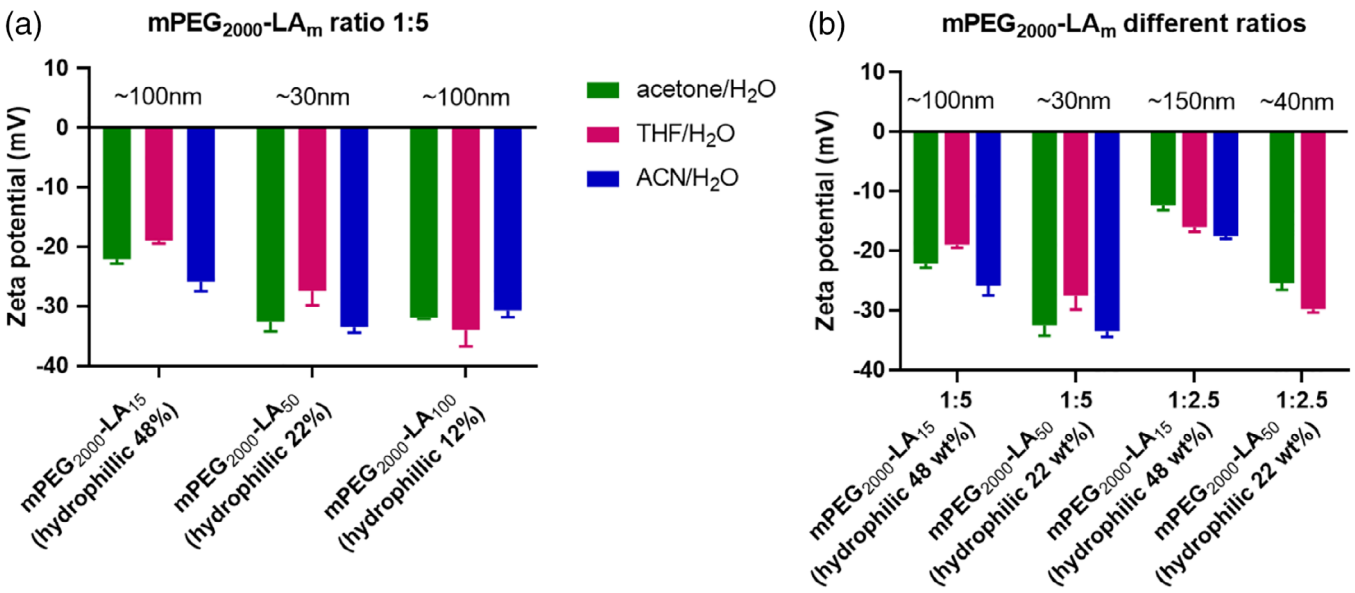


**FIGURE 5** Zeta potential measurements as an effect of hydrophilic:hydrophobic balance (length of mPEG initiator and units of LA) for the $mPEG_{2000}$ library when nanoformulated in three different solvents at different solvent:nonsolvent ratios into $H_2O$ (mean ± SD, error bars represent SD from three different measurements). Measurements were performed in pure water after full removal of the organic solvent (left) solvent:nonsolvent ratio of 1:5 (right) varied solvent ratios (approximate NP size indicated) [Color figure can be viewed at wileyonlinelibrary.com]

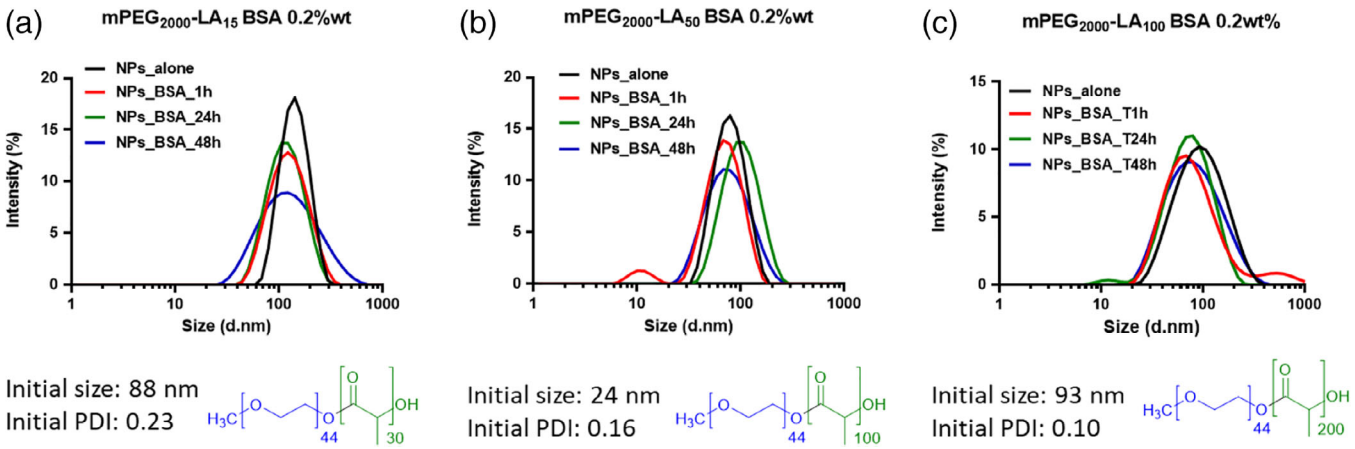


**FIGURE 6** Protein binding studies showing representative DLS traces of NPs after incubation in 0.2 wt% of BSA. NPs showed slight increases in size and broadening of the size distribution; however, no significant changes or aggregation was observed, confirming stability in these conditions. [Color figure can be viewed at wileyonlinelibrary.com]

reached only the same 87% final value. The higher concentration of salt required to effectively screen the surface charges for the more stable NPs was attributed to their higher charge density, and conversely, in the case of the $mPEG_{5000}$-$LA_{15}$, the NaCl was able to effectively screen the surface potential at a lower concentration.

The reported screening of NP formation and stability in this work has remarked not only the importance of the formulation strategy employed, but also the interplay among particle size, size distribution, and charge density to effectively link NP physical characteristics with stability in biologically relevant conditions.

## CONCLUSIONS

The present work investigated fundamental nanoformulation parameters such as the nature of organic solvent, nature of aqueous environment, ratio between solvent:nonsolvent, final NP concentration, reproducibility of hand-held simplified formulation strategies, as well as the ratio of hydrophobic:hydrophilic block of a small set of nanoformulated mPEG-PDLLA

copolymers. Understanding the behavior of these materials is of importance as they are chemical analogues of pharmaceutically relevant polymeric excipients used in commercial nanomedicines (Genexol-PM and Accurins). We undertook this systematic investigation to shed light on the nanoformulation parameters that influence NP physical properties and stability to guide future works in the field. It was observed that changing the organic solvent (acetone, THF, and ACN) and their ratio with regard to the aqueous phase ($H_2O$ and PBS) could significantly change the final NPs when the same polymer was used. It was confirmed that the amphiphilic balance of the copolymer influenced both the size and zeta potential of the NPs, and ultimately the stability to protein-induced aggregation in the presence of BSA, whereby block copolymers with small hydrophilic block% generally demonstrated improved NP stability. Taking into account the data reported, we have illustrated a methodological process to optimize important NPs parameters balancing particle size, size distribution, and surface charge, to ultimately generate stable and reproducible NPs based on PEG-PDLLA to guide future work within the nanoformulation field.

## ACKNOWLEDGMENTS

This work was supported by the Engineering and Physical Sciences Research Council [grant numbers (EPSRC; Grants EP/N006615/1 (AKP, CA), EP/N03371X/1 (VT, CA), EP/H005625/1 (CA), EP/L013835/1 (VT), and P/L015072/1 (PM, MM). This work was also funded by the Stoneygate Trust (CARO/SS/2018/PC2 (PM, MM) and the Royal Society (Wolfson Research Merit Award WM150086 (CA). The authors thank the Nanoscale and Microscale Research Centre (nmRC) at the University of Nottingham for providing access to TEM imaging. We also thank Prof. Rachel K. O'Reilly for her helpful and insightful comments.

## REFERENCES AND NOTES

**1** X. Xu, W. Ho, X. Zhang, N. Bertrand, O. Farokhzad, *Trends Mol. Med.* **2015**, *21*, 223.

**2** J. Shi, P. W. Kantoff, R. Wooster, O. C. Farokhzad, *Nat. Rev. Cancer* **2016**, *17*, 20.

**3** A. Kumari, S. K. Yadav, S. C. Yadav, *Colloids Surf. B Biointerfaces* **2010**, *75*, 1.

**4** H. S. Choi, W. Liu, P. Misra, E. Tanaka, J. P. Zimmer, B. I. Ipe, M. G. Bawendi, J. V. Frangioni, *Nat. Biotechnol.* **2007**, *25*, 1165.

**5** K. Raza, P. Kumar, N. Kumar, R. Malik, *Adv. Nanomed. Deliv. Ther. Nucleic Acids* **2017**, *5*(4), 166.

**6** J. Hrkach, D. Von Hoff, M. M. Ali, E. Andrianova, J. Auer, T. Campbell, D. De Witt, M. Figa, M. Figueiredo, A. Horhota, S. Low, K. McDonnell, E. Peeke, B. Retnarajan, A. Sabnis, E. Schnipper, J. J. Song, Y. H. Song, J. Summa, D. Tompsett, G. Troiano, T. V. G. Hoven, J. Wright, P. LoRusso, P. W. Kantoff, N. H. Bander, C. Sweeney, O. C. Farokhzad, R. Langer, S. Zale, *Sci. Transl. Med.* **2012**, *4*, 128ra39.

**7** J. Fang, H. Nakamura, H. A. Maeda, *Drug Deliv. Rev.* **2011**, *63*, 136.

**8** C. C. Fleischer, C. K. Payne, *Acc. Chem. Res.* **2014**, *47*, 2651.

**9** T. P. Padera, B. R. Stoll, J. B. Tooredman, D. Capen, E. Di Tomaso, R. K. Jain, *Nature* **2004**, *427*, 695.

**10** R. K. Jain, T. Stylianopoulos, *Nat. Rev. Clin. Oncol.* **2010**, *7*, 653.

**11** M. R. Dreher, W. Liu, C. R. Michelich, M. W. Dewhirst, F. Yuan, A. J. N. Chilkoti, *Cancer Inst.* **2006**, *98*, 335.

**12** Z. Popović, W. Liu, V. P. Chauhan, J. Lee, C. Wong, A. B. Greytak, N. Insin, D. G. Nocera, D. Fukumura, R. K. Jain, M. G. A. Bawendi, *Chem. Int. Ed.* **2010**, *49*, 8649.

**13** S. C. Kim, D. W. Kim, Y. H. Shim, J. S. Bang, H. S. Oh, S. W. Kim, M. H. Seo, *J. Control. Release* **2001**, *72*, 191.

**14** S. Ashton, Y. H. Song, J. Nolan, E. Cadogan, J. Murray, R. Odedra, J. Foster, P. A. Hall, S. Low, P. Taylor, R. Ellston, U. M. Polanska, J. Wilson, C. Howes, A. Smith, R. J. A. Goodwin, J. G. Swales, N. Strittmatter, Z. Takáts, A. Nilsson, P. Andren, D. Trueman, M. Walker, C. L. Reimer, G. Troiano, D. Parsons, D. De Witt, M. Ashford, J. Hrkach, S. Zale, P. J. Jewsbury, S. T. Barry, *Sci. Transl. Med.* **2016**, *8*, 325ra17.

**15** W. W. Gerhardt, D. E. Noga, K. I. Hardcastle, A. J. García, D. M. Collard, M. Weck, *Biomacromolecules* **2006**, *7*, 1735.

**16** B. Jeong, Y. H. Bae, D. S. Lee, S. W. Kim, *Nature* **1997**, *388*, 860.

**17** K. J. Zhu, L. Xiangzhou, Y. Shilin, *J. Appl. Polym. Sci.* **1990**, *39*, 1.

**18** H. Qian, A. R. Wohl, J. T. Crow, C. W. MacOsko, T. R. Hoye, *Macromolecules* **2011**, *44*, 7132.

**19** L. A. Ruiz-Cantu, A. K. Pearce, L. Burroughs, T. M. Bennett, C. E. Vasey, R. Wildman, D. J. Irvine, C. Alexander, V. Taresco, *Macromol. Chem. Phys.* **2019**, *220*, 1800459.

**20** C. E. Vasey, A. K. Pearce, F. Sodano, R. Cavanagh, T. Abelha, V. Cuzzucoli Crucitti, A. B. Anane-Adjei, M. Ashford, P. Gellert, V. Taresco, C. Alexander, *Biomater. Sci.* **2019**. Advance Article. https://doi.org/10.1039/C9BM00667B

**21** B. G. G. G. Lohmeijer, R. C. Pratt, F. Leibfarth, J. W. Logan, D. A. Long, A. P. Dove, F. Nederberg, J. Choi, C. Wade, R. M. Waymouth, J. L. Hedrick, *Macromolecules* **2006**, *39*, 8574.

**22** W. Chin, G. Zhong, Q. Pu, C. Yang, W. Lou, P. F. De Sessions, B. Periaswamy, A. Lee, Z. C. Liang, X. Ding, S. Gao, C. W. Chu, S. Bianco, C. Bao, Y. W. Tong, W. Fan, M. Wu, J. L. Hedrick, Y. Y. Yang, *Nat. Commun.* **2018**, *9*, 917.

**23** A. Baroni, L. Vlaminck, L. Mespouille, F. Du Prez, N. Delbosc, B. Blankert, *Macromol. Rapid Commun.* **2019**, *40*, 1800743.

**24** S. S. Yu, C. M. Lau, S. N. Thomas, W. Gray Jerome, D. J. Maron, J. H. Dickerson, J. A. Hubbell, T. D. Giorgio, *Int. J. Nanomedicine* **2012**, *7*, 799.

**25** J. M. Rabanel, J. Faivre, S. F. Tehrani, A. Lalloz, P. Hildgen, X. Banquy, *ACS Appl. Mater. Interfaces* **2015**, *7*, 10374.

**26** A. M. de Oliveira, E. Jäger, A. Jäger, P. Stepánek, F. C. Giacomelli, *Colloids Surf. A Physicochem. Eng. Asp.* **2013**, *436*, 1092.

**27** W. Huang, C. Zhang, *Biotechnol. J.* **2018**, *13*, 1700203.

**28** C. Pucci, F. Cousin, F. Dole, J. P. Chapel, C. Schatz, *Langmuir* **2018**, *34*, 2531.

**29** M. Beck-Broichsitter, J. Nicolas, P. Couvreur, *Nanoscale* **2015**, *7*, 9215.

**30** M. Bagheri, J. Bresseleers, A. Varela-Moreira, O. Sandre, S. A. Meeuwissen, R. M. Schiffelers, J. M. Metselaar, C. F. Van Nostrum, J. C. M. Van Hest, W. E. Hennink, *Langmuir* **2018**, *34*, 15495.

**31** T. K. Endres, M. Beck-Broichsitter, O. Samsonova, T. Renette, T. H. Kissel, *Biomaterials* **2011**, *32*, 7721.

**32** I. D. Styliari, C. Conte, A. K. Pearce, A. Hüsler, R. J. Cavanagh, M. J. Limo, D. Gordhan, A. Nieto-Orellana, J. Suksiriworapong, B. Couturaud, P. Williams, A. L. Hook,

M. R. Alexander, M. C. Garnett, C. Alexander, J. C. Burley, V. Taresco, *Macromol. Mater. Eng.* **2018**, *303*, 1800146.

**33** S. Patil, A. Sandberg, E. Heckert, W. Self, S. Seal, *Biomaterials* **2007**, *28*, 4600.

**34** N. Schultz, G. Metreveli, M. Franzreb, F. H. Frimmel, C. Syldatk, *Colloids Surf. B Biointerfaces* **2008**, *66*, 39.

**35** C. Graf, Q. Gao, I. Schütz, C. N. Noufele, W. Ruan, U. Posselt, E. Korotianskiy, D. Nordmeyer, F. Rancan, S. Hadam, A. Vogt, J. Lademann, V. Haucke, E. Rühl, *Langmuir* **2012**, *28*, 7598.

**36** D. S. Nikam, S. V. Jadhav, V. M. Khot, R. S. Ningthoujam, C. K. Hong, S. S. Mali, S. H. Pawar, *RSC Adv.* **2014**, *4*, 12662.